Spectral narrowing of x-ray pulses for precision spectroscopy with nuclear resonances

K. P. Heeg,[1] A. Kaldun,[1] C. Strohm,[2] P. Reiser,[1] C. Ott,[1] R. Subramanian,[1] D. Lentrodt,[1] J. Haber,[2] H.-C. Wille,[2] S. Goerttler,[1] R. Rüffer,[3] C. H. Keitel,[1] R. Röhlsberger,[2] T. Pfeifer,[1] J. Evers[1*]

[1]Max-Planck-Institut für Kernphysik, Saupfercheckweg 1, 69117 Heidelberg, Germany
[2]Deutsches Elektronen-Synchrotron DESY, Notkestraße 85, 22607 Hamburg, Germany
[3]ESRF-The European Synchrotron, CS40220, 38043 Grenoble Cedex 9, France

[*]E-mail: joerg.evers@mpi-hd.mpg.de

Spectroscopy of nuclear resonances offers a wide range of applications due to the remarkable energy resolution afforded by their narrow linewidths. However, progress to higher resolution is inhibited at modern x-ray sources, since they deliver only a tiny fraction of the photons on resonance, while the majority contributes to an off-resonant background. We use the fast mechanical motion of a resonant target to manipulate the spectrum of a given x-ray pulse and to redistribute off-resonant spectral intensity onto the resonance. As a consequence, the resonant pulse brilliance is increased, while the off-resonant background is reduced. As our method is compatible with existing and upcoming pulsed x-ray sources, we anticipate that this approach will find applications requiring ultra-narrow x-ray resonances.

Due to the Mössbauer effect (*1*), nuclei may absorb and emit photons without appreciable

recoil, giving rise to extremely narrow resonance widths. This narrow linewidth provides the basis to most applications of Mössbauer spectroscopy, which is a well-established tool to measure magnetic, structural and dynamic properties of matter (*2*). It also provides a natural platform for various fundamental tests (*1, 3–5*). Further applications include the study of solid state phenomena (*6*), battery development (*7*) and x-ray quantum optics (*8–13*). Most experiments use measurements on the ^{57}Fe Mössbauer nuclear resonance, for which the energy resolution $\Delta E/E$ defined as the ratio of transition linewidth and energy is 3×10^{-13}. The achievable energy resolution could even increase by orders of magnitude with other Mössbauer isotopes, such as ^{45}Sc ($\Delta E/E \sim 10^{-19}$), ^{107}Ag and ^{109}Ag ($\Delta E/E \sim 10^{-22}$), or ^{103}Rh ($\Delta E/E \sim 10^{-24}$) (*1*). Even though the brilliance of pulsed x-ray sources is much higher than that of radioactive sources, it needs to be boosted further for metrology with these ultranarrow resonances. Furthermore, higher signal rates translate into better energy, temporal, or spatial resolution (*1*), such that more efficient excitation of narrow resonances could also advance their applications in general. On the other hand, broader transitions are suitable candidates for realizing nonlinear effects in the x-ray regime (*12, 14–16*).

Unfortunately, state-of-the-art pulsed x-ray sources provide radiation with bandwidths orders of magnitude larger than the nuclear resonances. Monochromators only remove off-resonant background photons, but cannot enhance the resonant component. Attempts to create spectrally narrow x-rays via γ-ray lasers have proven unsuccessful so far (*17, 18*).

We propose a different approach, which neither increases the total x-ray intensity, nor directly creates narrow-band x-ray light. Instead, we manipulate the spectra of given broadband x-ray pulses, such that off-resonant parts are shifted onto resonance (Fig. 1A). The incident pulse is spectrally broad compared to the displayed frequency range, and we normalize its spectrum to unity. The interaction with a static target containing a narrow nuclear resonance imprints an absorption dip onto this input spectrum. We control this interaction in the time domain, such

that instead, the transmitted light on resonance exceeds the input spectral intensity, while off-resonant parts of the spectrum are further attenuated to satisfy energy conservation. This effect can be strong enough to over-compensate all other sources of losses in the setup, including broadband electronic absorption. As a result, the resonant x-ray intensity downstream of our setup is increased compared to the incoming x-ray pulse.

The required strong manipulations of the nuclei are typically unfeasible, e.g., since suitable external electromagnetic control fields are generally unavailable for nuclei. One can overcome this lack using mechanical control instead (*19, 20*). Here we exploit precise mechanical displacements of the target via a piezoelectric transducer (Fig. 1B). Immediately after excitation by a short x-ray pulse, a displacement $x(t)$ is applied to the target while it re-emits x-rays. Compared to the target at rest, the scattered field will then carry the translational phase $\exp\left[ikx(t)\right]$. While the temporal intensity dependence of the detected x-rays remains unaffected, their spectral composition is redistributed (*21*).

The increased resonant x-ray intensity illustrated in Fig. 1A is achieved via a step-like piezo displacement by half the resonant x-ray wavelength that shifts the phase of the scattered light by π and converts the usual destructive interference with the non-interacting x-rays into constructive interference (*22*) (the optimal displacement is discussed in (*21*)). The spectral redistribution is apparent from the stronger absorption away from resonance (Fig. 1B and (*21*)). Related piezo techniques have been used before to shape single narrow-band γ-ray photons in the time domain (*10, 23–26*). Also broadband x-ray pulses (*27*) have been considered, but spectral shaping (*28*) has received little attention so far.

We implemented our scheme using the Mössbauer isotope ^{57}Fe with its nuclear transition at energy $\hbar\omega_0 = 14.4$ keV. The resonance width of $\hbar\gamma = 4.7$ neV corresponds to a lifetime of 141 ns, during which a controlled piezo displacement is experimentally feasible. The experiments were performed at the synchrotron sources ESRF (Grenoble, France) and PETRA III

(DESY Hamburg, Germany). The target mounted on the piezo consists of α-iron with thickness 2 μm, enriched in the resonant isotope ^{57}Fe to 95%. The magnetization was externally aligned such that two magnetic hyperfine transitions were driven by the x-rays. The piezo motion was controlled via an arbitrary-function generator (*21*). Triggered by the synchrotron bunch clock, each x-ray pulse is manipulated by the same piezo motion, such that the desired resonant brilliance boost can be observed in the data averaged over all x-ray pulses.

For energy analysis of the radiation transmitted through the piezo target, we used a single-line reference absorber consisting of ^{57}Fe-enriched stainless steel, mounted on a Doppler drive, and scanned it across the ^{57}Fe resonance (see Fig. 2A and (*21*)). The analysis of the combined temporal response of target and analyzer provides access to both the piezo motion and the generated x-ray spectra. A subset of such time- and energy-dependent measurements integrated over different detection time windows is shown in Fig. 2C. The actual motion of the target on the piezo does not directly follow the applied voltage signal, most likely due to signal dispersion and bandwidth limitations in the transmission from electric voltage to mechanical motion. To determine the piezo motion, we used an evolutionary algorithm in which an initially random motion without assuming a particular motional pattern was successively optimized towards best agreement between simulation and measured data (*21*). The resulting converged theoretical curves are shown as solid lines in Figs. 2C, and the reconstructed piezo motions in Fig. 2B. The reconstructed motion then allows us to calculate the generated x-ray spectra via a Fourier transform of the phase-modulated pulses.

In the x-ray pulse spectra normalized to the input spectra (Fig. 2D), obtained for the displacements shown in Fig. 2B, the black colored spectrum is a reference without piezo motion. Off resonance, its normalized spectral intensity is below unity because of electronic absorption. With motion of the target (red, blue), the resonant intensity clearly exceeds that of the incident pulse by more than a factor of 3. The spectral rearrangement is confirmed by the fact

that the motion shown in blue rearranges lower spectral regions onto the respective resonances, whereas the opposite motion shown in red shuffles higher frequencies onto resonance (see arrows). These main spectral features are already well visible in the experimental raw data integrated over late photon arrival times (lower panel of Fig. 2C), which approximates the spectrum of the piezo target alone (*8, 13*). The properties of the generated x-rays closely resemble those of ideal narrow-band pulses, as can be seen in their respective Wigner representations (Fig. S7 in (*21*)). Our theoretical analysis (*21*) shows that an enhancement factor of 12 is possible for a single α-iron foil with optimized thickness.

To investigate the possibility of further enhancement, we performed proof-of-principle experiments with two piezo stages, which also allowed for stringent tests of the recovered piezo motions. Enhancements beyond the single piezo capabilities are possible if multiple piezos harvest intensity from different off-resonant spectral regions. In our experiment shown in Fig. 3A, the two piezos harvest from spectral regions above and below the resonance, respectively. We first individually reconstructed the respective motions of the two piezos (Fig. 3B). Then, we theoretically optimized the resonant intensity boost expected for both piezos combined by temporally shifting their motions relative to the synchrotron bunch clock. The subsequent optimized measurement with two piezo stages shows good agreement with the theoretical predictions (Fig. 3C). This also confirms the recovered piezo motions, since the theoretical predictions for two piezos were based on the single-stage measurements only. Note that multiple piezos have also been studied with narrow-band γ-ray sources (*29*).

These results readily open the way for more general manipulations of the spectrum. Similar brilliance enhancements with a single-line spectrum as in Fig. 1 are feasible with suitable single-line targets, e.g., stainless steel enriched in ^{57}Fe. We have verified this by calculating the resonant enhancement expected with the single-line absorber and the motional pattern used in our experiment. In additional experiments, we investigated piezo motions with larger ampli-

tude, which redistribute intensity over a wider spectral range (See (*21*)). Note that the partial longitudinal coherence of synchrotron or XFEL pulses is not a limitation for switching times on the order of nanoseconds (See (*21*)). It may be possible to cascade even more piezo stages, further increasing the resonant x-ray brilliance. Extensions of this scheme can be envisioned by replacing the piezo-based mechanical displacement with faster laser-induced phononic control of the positions of the nuclei. More general time-dependent displacements could facilitate the engineering of arbitrary spectra. This provides a direct link to laser pulse shaping, a widespread technique in ultrafast optics with many applications (*30*). Ultimately, closed-loop feedback setups could be envisioned to optimize the x-ray pulse spectra for specific applications, such as selective excitations in compound materials, or enhanced non-linear light-matter interactions. These perspectives reach beyond Mössbauer resonances, since our method is general and applies to spectroscopy in general. On the other hand, the possibility to track motion on sub-Å scales with short and focused x-ray beams developed here could serve as a valuable tool in a wide range of scientific applications, e.g., to study laser-induced mechanical excitations or distortions with high spatial and temporal resolution.

References and Notes

1. M. Kalvius, P. Kienle, eds., *The Rudolf Mössbauer Story* (Springer, Heidelberg, 2012).

2. R. Röhlsberger, *Nuclear Condensed Matter Physics with Synchrotron Radiation* (Springer, Berlin Heidelberg, 2005), vol. 208 of *Springer Tracts in Modern Physics*.

3. R. V. Pound, G. A. Rebka, *Phys. Rev. Lett.* **3**, 439 (1959).

4. D. C. Champeney, G. R. Isaak, A. M. Khan, *Nature* **198**, 1186 (1963).

5. K. C. Turner, H. A. Hill, *Phys. Rev.* **134**, B252 (1964).

6. I. Troyan, *et al.*, *Science* **351**, 1303 (2016).

7. L. Jun, W. Tianpin, A. Khalil, *Nature Energy* **2**, 17011 (2017).

8. R. Röhlsberger, K. Schlage, B. Sahoo, S. Couet, R. Rüffer, *Science* **328**, 1248 (2010).

9. R. Röhlsberger, H.-C. Wille, K. Schlage, B. Sahoo, *Nature* **482**, 199 (2012).

10. F. Vagizov, V. Antonov, Y. V. Radeonychev, R. N. Shakhmuratov, O. Kocharovskaya, *Nature* **508**, 80 (2014).

11. K. P. Heeg, *et al.*, *Phys. Rev. Lett.* **111**, 073601 (2013).

12. K. P. Heeg, *et al.*, *Phys. Rev. Lett.* **114**, 203601 (2015).

13. K. P. Heeg, *et al.*, *Phys. Rev. Lett.* **114**, 207401 (2015).

14. T. E. Glover, *et al.*, *Nature* **488**, 603 (2012).

15. S. Shwartz, *et al.*, *Phys. Rev. Lett.* **112**, 163901 (2014).

16. K. Tamasaku, *et al.*, *Nat Photon* **8**, 313 (2014).

17. G. C. Baldwin, J. C. Solem, *Rev. Mod. Phys.* **69**, 1085 (1997).

18. E. V. Tkalya, *Phys. Rev. Lett.* **106**, 162501 (2011).

19. D.-W. Wang, *et al.*, *Phys. Rev. Lett.* **110**, 093901 (2013).

20. D. Mukhopadhyay, *et al.*, *Nat Commun* **6**, 7057 (2015).

21. See Supplemental Material at URL.

22. C. Ott, *et al.*, *Science* **340**, 716 (2013).

23. P. Helistö, I. Tittonen, M. Lippmaa, T. Katila, *Phys. Rev. Lett.* **66**, 2037 (1991).

24. R. N. Shakhmuratov, F. Vagizov, O. Kocharovskaya, *Phys. Rev. A* **84**, 043820 (2011).

25. R. N. Shakhmuratov, *et al.*, *Phys. Rev. A* **92**, 023836 (2015).

26. Y. V. Radeonychev, V. A. Antonov, F. G. Vagizov, R. N. Shakhmuratov, O. Kocharovskaya, *Phys. Rev. A* **92**, 043808 (2015).

27. P. Schindelmann, *et al.*, *Phys. Rev. A* **65**, 023804 (2002).

28. P. Schindelmann, Kernresonante Vorwärtsstreuung von Mößbauer- und Synchrotronstrahlung unter dem Einfluß von Ultraschall, Ph.D. thesis, Technische Universität München, Allensbach (1999).

29. R. N. Shakhmuratov, F. Vagizov, O. Kocharovskaya, *Phys. Rev. A* **87**, 013807 (2013).

30. A. Weiner, *Ultrafast Optics* (John Wiley & Sons, Inc., Hoboken, New Jersey, 2009).

31. P. Reiser, Time domain control of x-ray quantum dynamics, Master's thesis, Ruprecht-Karls-Universität Heidelberg (2014).

32. W. Sturhahn, *Hyperfine Interactions* **125**, 149 (2000).

33. T. Pfeifer, Y. Jiang, S. Düsterer, R. Moshammer, J. Ullrich, *Opt. Lett.* **35**, 3441 (2010).

34. H.-C. Wille, H. Franz, R. Röhlsberger, W. A. Caliebe, F.-U. Dill, *Journal of Physics: Conference Series* **217**, 012008 (2010).

35. R. Rüffer, A. I. Chumakov, *Hyperfine Interactions* **97-98**, 589 (1996).

Acknowledgments

We acknowledge a consolidator grant from the European Research Council (ERC) (X-MuSiC-616783). This work is part of and supported by the DFG Collaborative Research Centre "SFB 1225 (ISOQUANT)." We acknowledge the support of the Helmholtz Association through project-oriented funds. The authors declare no competing financial interest.

Supplementary Materials

Supplementary Text

Figs. S1-S7

References (*31–35*)

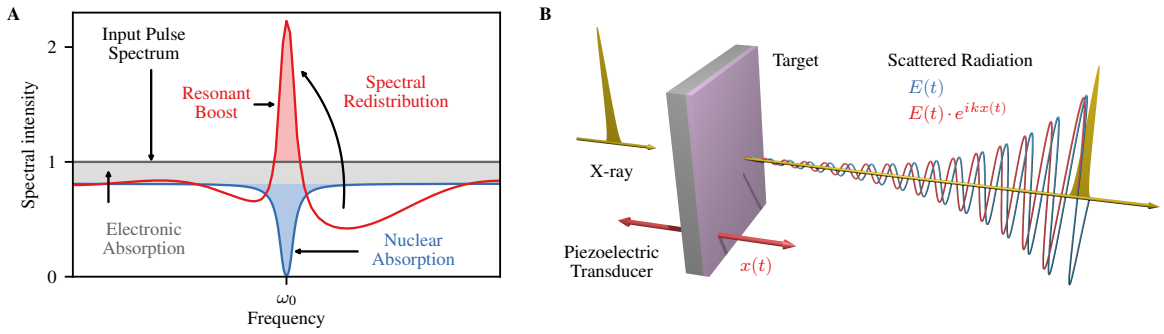

Figure 1: Increasing the resonant x-ray brilliance. A The interaction of x-rays with a static target containing a narrow resonance usually imprints a resonant absorption dip onto the spectrum, accompanied by broadband electronic absorption (blue curve, compared to the dark gray normalized input spectrum). Here, we manipulate this interaction such that off-resonant photons are redistributed onto resonance. As a consequence, the resonant intensity of the x-rays is substantially enhanced, while the undesired off-resonant background is reduced (red curve). **B** This manipulation is achieved by mechanically displacing the target immediately after excitation. With motion (red), a time-dependent phase is imprinted onto the scattered light (blue). This modifies the interference with the unscattered light (yellow), enabling one to tailor the spectrum of the resulting x-ray pulse.

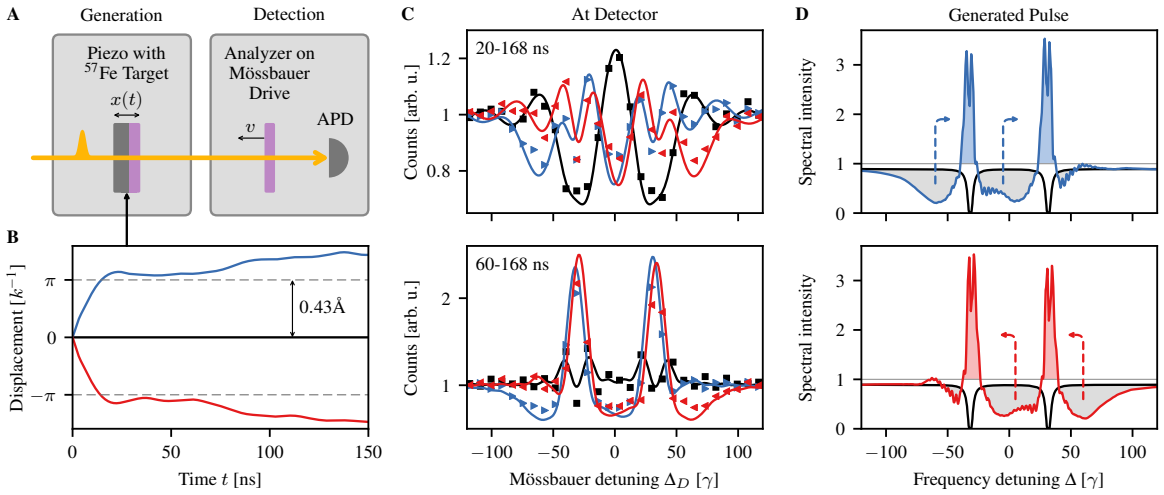

Figure 2: Experimental setup and results. **A** Short x-ray pulses (yellow) impinge on a ^{57}Fe target (purple), which is displaced immediately after excitation by a piezo (gray). As spectral analyzer, we used a ^{57}Fe single-line absorber on a Doppler drive, which allowed us to adjust the detuning Δ_D between target and analyzer via its velocity v. **B** Two approximately opposite piezo motions (red, blue) as function of time, reconstructed from the measurements. **C** Selection of spectra recorded as a function of Δ_D. Data is shown for the two motions from **B** (blue, red) and for the target at rest (black), with theoretical fits (solid lines). The two panels differ in the integration range over photon arrival times after the excitation. Photon shot noise errors are within the marker size. **D** Reconstructed x-ray pulse spectra behind the piezo target. Without motion, two hyperfine absorption lines are obtained (black). With motion, the spectral intensity significantly exceeds the incident intensity on resonance (blue, red; colors as in **B** and **C**). Gray shaded areas indicate regions out of which spectral intensity is redistributed onto resonance.

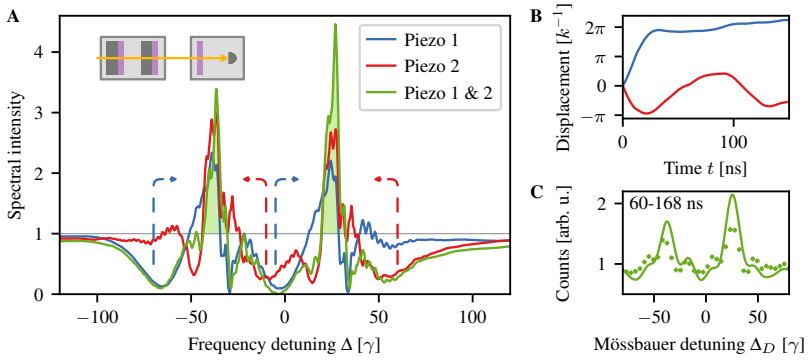

Figure 3: Cascading two piezo stages. A Spectrum generated with two ^{57}Fe targets on separate piezo stages (green), and the corresponding spectra for the respective single piezo stages (red, blue). **B** The two respective motional patterns redistribute spectral power from different off-resonant regions onto resonance (dashed arrows in **A**). Thus, the combination of the two stages increases the resonant intensity beyond what is achieved with a single piezo (red, blue). **C** Measured spectrum for the two-piezo setup, and corresponding theoretical prediction (solid line). Photon shot noise errors are within the marker size.